Journal of Environmental Statistics

Sep 2019, Volume 9, Issue 4. http://www.jenvstat.org

Statistical Surveillance Thresholds for Enhanced Situational Awareness of Spring Wildland Fire Activity in Alberta, Canada

Cordy Tymstra
Department of Renewable Resources
University of Alberta

Douglas G. Woolford
Department of Statistical and Actuarial Sciences
University of Western Ontario

Mike D. Flannigan
Department of Renewable Resources
University of Alberta

Abstract

Wildland fire disasters across Canada and globally are increasing in frequency. Alberta's spring wildfire season is a particularly challenging period. Situational awareness of the wildfire environment is critical for wildfire management agencies to be prepared when extreme events occur. We propose the use of simple initial attack (IA) and being held (BH) escape surveillance charts in near-real time with thresholds as tools for enhancing and tracking situational awareness. Since the discrete data sets we used are zero-inflated and over-dispersed we chose to model the exceedances over a threshold. We also used preceding December sea surface temperatures (SST) of the Pacific Ocean as an indicator of persistent spring wildfire activity. Our analysis indicates the tracking of IA and BH escapes and SST can provide additional decision support as part of an early warning system of spring wildfire risk.

Keywords: early warning system, extreme events, peak over threshold, wildfire escapes.

1. Introduction

Natural disasters and catastrophes[1] are increasing globally in frequency, and cost. Based on insured losses in 2017, wildfires worldwide totaled a record $14.62 billion USD, and in California, United States alone they resulted in the fourth costliest natural catastrophe ($12 billion USD) (Swiss Re Institute 2018). British Columbia, Canada also experienced a disastrous

[1]Major disasters resulting in $25 million or more in insured property losses (Insurance Information Institute 2018)

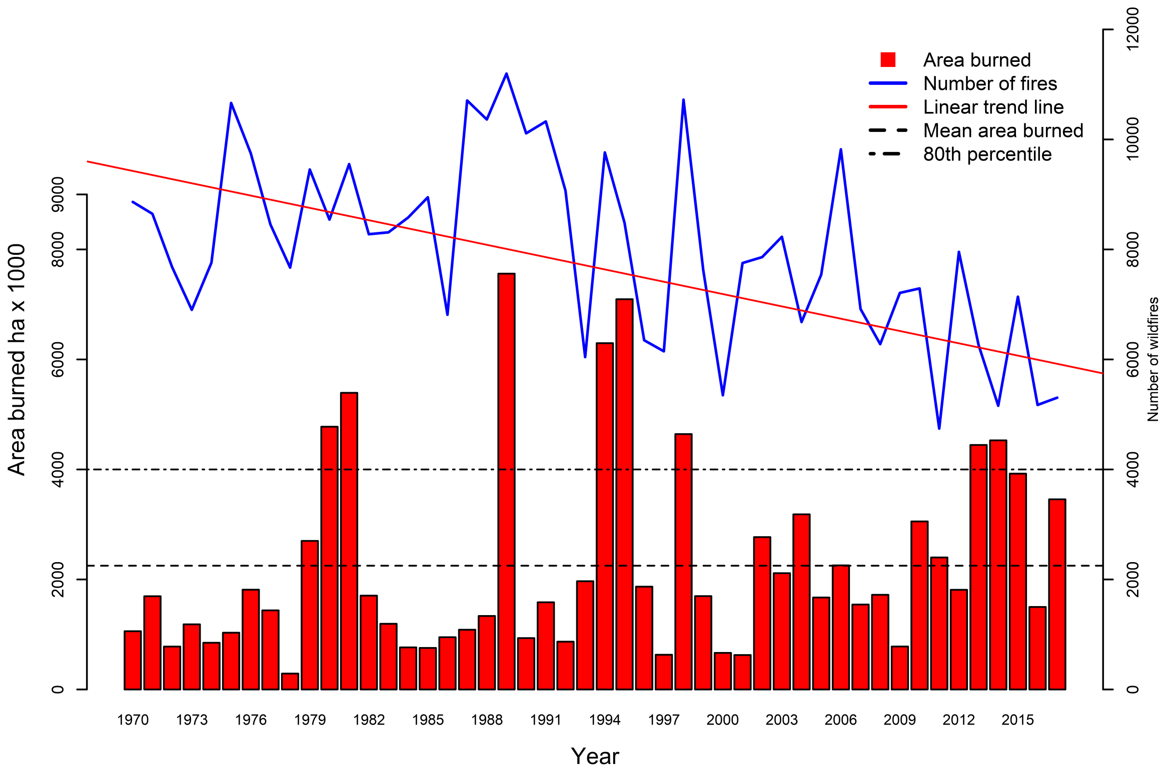

Figure 1: The annual number of wildland fires and total area burned in Canada over the period 1970 - 2017.

wildfire season in 2017 when 1,351 wildfires burned a record 1.2 million ha and displaced 65,000 residents (Abott and Chapman 2018). In 2016, the 589,552 ha Horse River Wildfire in Alberta, Canada resulted in insurance claims totalling $3.7 billion (Insurance Bureau of Canada 2017).

Large wildfires are not uncommon in Canada, particularly in the boreal forest (Tymstra 2015). On average Canada experiences 8,000 wildfires and 2.25 million ha burned each year. Historically, about 20% of the time the total annual area burned has exceeded 4 million ha (80^{th} percentile) (Figure 1). A commonly used definition for a large wildfire in Canada is a wildfire whose final size was 200 ha or more (Stocks *et al.* 2002); Only 4% of wildfires in Canada exceed 200 ha in size but they account for about 99% of the total area burned.

Although the number of wildfires in Canada, with a few regional exceptions, has been trending downward, the number of wildfire disasters have been trending upward by decade since 1980 (Public Safety Canada 2018). During the 2010 - 2017 period 78% of the national burned area occurred in western Canada (Yukon Territory, Northwest Territories, British Columbia, Alberta and Saskatchewan) (Natural Resources Canada 2018).

Early warning of fire danger conditions is critical to ensure preparedness activities contribute to preventing and mitigating wildfire disasters. Situational awareness requires having a perception and comprehension of the current situation and then projecting it into the future to provide early warning and preparedness decision support (Endsley 1995). Since it can take two weeks or longer to mobilize resources from other countries, wildfire management agencies need a situational awareness based on 10 - 14 day outlooks of weather and fire occurrence. The foundation for early wildfire danger warning in Canada is the Canadian Forest Fire Danger Rating System (CFFDRS) (Stocks *et al.* 1989; de Groot *et al.* 2015). The two main components of the CFFDRS are the Fire Weather Index (FWI) Subsystem which is widely applied around the world (de Groot *et al.* 2015), and the Fire Behaviour Prediction (FBP) Subsystem. The FWI Subsystem provides a relative rating of fuel moisture codes representing fuel layers, and fire behaviour indices. The FBP Subsystem incorporates the FWI System outputs to provide quantitative assessments of fire behaviour for specific fuel types across Canada.

Assessing wildfire environment conditions in early spring solely using the CFFDRS outputs can be a challenge if the full complement of weather stations are not yet operational. Since the CFFDRS fuel moisture codes are not direct measurements of the fuel layers, fuel moisture code validation may be necessary to adequately account for the over-winter precipitation effect on fuel moisture, and accurately start the FWI fuel moisture codes in the spring. Foliar moisture content too, can influence spring wildfire behavior, but the default date for minimum Foliar Moisture Content (FMC) may be inaccurate because the actual date of minimum FMC can shift up to 4 - 5 weeks from year to year (Van Wagner 1967).

The spring season can therefore be a particularly challenging wildfire danger period for wildfire management agencies across Canada. In Alberta, disastrous spring wildfire seasons occurred in 1995, 1998, 2001, 2002, 2011 and 2016 when environmental conditions (low foliar moisture content, no green-up, low relative humidity, and strong, dry winds) supported extreme wildfire behaviour (Figure 2). Wildfire starts in Alberta during the month of May alone accounted for 23% of the total number of wildfires, and 51% of the total area burned for the entire wildfire season (March 1 - October 31) from 1990 to 2017. Most (81%) of the May wildfire starts are human-caused.

There is subsequently a strong need to develop tools in addition to the CFFDRS to provide enhanced situational awareness during the challenging spring wildfire period between snowmelt and green-up. Our work is motivated by what appears in the health sciences literature, including the various approaches and statistical models used to forecast disease outbreaks. Examples include generalized linear modeling (Goldstein *et al.* 2011), hierarchical statistical modeling (Mugglin *et al.* 2002), and autoregressive integrated moving average modeling (ARIMA) with climatological parameters (Soebiyanto *et al.* 2010) for predicting influenza outbreaks; logistic regression modeling for West Nile Virus incidence prediction; statistical/machine learning using least absolute shrinkage and selection operator (LASSO) methods (Shi *et al.* 2016), Knorr-Held two-component (K-H) modeling (Earnest *et al.* 2012), and Poisson multivariate regression modeling (Hii *et al.* 2012) for predicting dengue fever. Thomson and Mason (2012) used seasonal climate forecasts from multi-modal ensembles to predict malaria outbreaks. Surrogate data such as social media (Yang *et al.* 2013), over-the-counter drug sales (Das *et al.* 2005), and absenteeism in school (Kara *et al.* 2011), have also been used to predict infectious disease outbreaks.

Unlike disease surveillance and other biosurveillance methods and applications, the literature on statistical approaches applied to provide early warning of potential surges in wildfire activity, is comparatively sparse. Taylor *et al.* (2013) summarized the methods used to predict

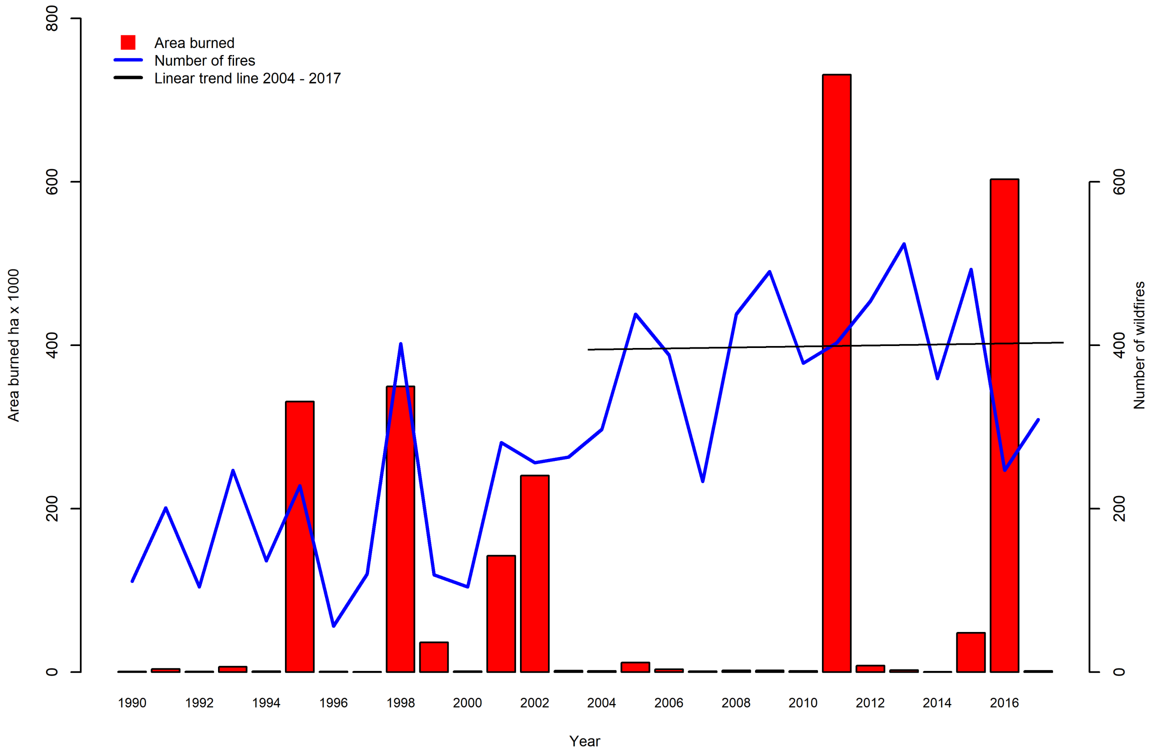

Figure 2: Annual total number of wildfire starts in May and the corresponding total area burned from these wildfire starts in Alberta over the period 1990 - 2017. A linear trend line for the number of wildland fire starts is also shown, starting from 2004 when reporting procedures changed.

wildfire occurrence (arrival) and wildfire behavior (growth). Examples of statistical methods used to provide wildfire management decision support include the estimation of wildfire risk using probability based models (Preisler *et al.* 2004); application of a mixture modeling framework to monitor historical trends in lightning wildfire risk (Woolford *et al.* 2014); development of an early warning wildfire risk system based on modelling vegetation green-up using satellite observations (Pickell *et al.* 2017); and the use of machine learning (artificial neural network) to predict weather patterns associated with extreme wildfire events (Lagerquist *et al.* 2017).

The objectives of this paper are to conduct an exploratory analysis of historical wildland fire records to examine methods for short-term situational awareness and to explore for possible teleconnection signals between pre-fire season sea surface temperatures (SST) and characteristics of wildfire activity in the spring. Our study region is the entire legislated Forest Protection Area in Alberta over the period 1990 to 2015 (Figure 3).

We focus our exploratory analysis on process control and the operational application of control charts. Syndromic surveillance (Fricker 2013) with statistical thresholds is shown to be a viable approach to enhance the situational awareness of potential spring wildfire activity in Alberta. Syndromic surveillance uses nowcasting data to continuously monitor, analyze, and detect data aberrations that signal a current or likely event change.

Figure 3: Forest Protection Area within the Province of Alberta, Canada.

We also explore the application of a simple metric to forecast the persistence of spring wildfire activity in Alberta based on the association between December sea surface temperature anomalies in the south-east Pacific Ocean, and wildfire activity in the spring. When the predominantly eastern trade winds over the south-east Pacific ocean weaken, warm water flows in a reverse west to east pattern (Rasmusson and Wallace 1983). This phenomena, called El Niño, causes a shift in atmospheric circulation which influences weather patterns. In western Canada this results in above average temperatures in the winter and spring.

We hypothesize that during such ENSO (El Niño Southern Oscillation) warming events the wildfire activity in early spring is an indicator of persistent wildfire activity into late spring. Skinner *et al.* (2006) reported a positive correlation between ENSO and the Pacific Decadal Oscillation (PDO),and Shabbar *et al.* (2011) found a lagged association of forest fire severity conditions with ENSO warming events across Canada's boreal forest. Beverly *et al.* (2011) also found a coupling of the large wildfire activity in Canada with the Arctic Multidecadal Oscillation (AMO). They suggested that wind may be a critical component of this coupling. At a provincial level, wildfire activity in British Columbia was correlated positively with ENSO and PDO indices (Wang *et al.* 2010).

2. Data

2.1. Initial Attack and Being Held Escapes

When initial attack (IA) resources are dispatched to a wildfire in Alberta, the objective is to initiate suppression activities before the wildfire exceeds 2.0 ha in size. Wildfires that exceed 2.0 ha in size before IA resources arrive are referred to as IA escapes. If a wildfire can be contained by 1000 h the day following its initial assessment, a second objective called Being Held (BH) is achieved. Wildfires with a BH status are not expected to increase in size based on the current fire environment conditions. If the BH objective is not attained the wildfire is referred to as a BH escape (Government of Alberta 2018a).

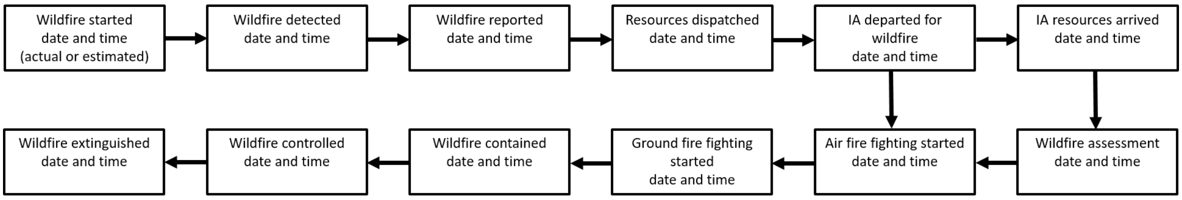

Figure 4: Wildfire attribution in Alberta's FIRES system from ignition to extinguishment.

The IA and BH attribute data, and other data characterizing a wildfire from ignition to extinguishment (Figure 4) are entered in near-real time in a system used in Alberta called FIRES (Fire Information and Resource Environment System). Data entry into FIRES began in 1990. Exported data from FIRES were obtained from the Wildfire Management Branch for the 1990 - 2017 period. We reserved the years 2016 and 2017 for model testing purposes.

In 1995, the minimum reporting wildfire size was reduced from 0.1 ha to 0.01 ha. Then in 2004, the reporting procedure changed to include permit related Order to Remove (OTR) wildfires (usually residents using burn barrels) and abandoned illegal campfires (called XA wildfires) that took less than 15 minutes to extinguish. An increase in the number of reported wildfires beginning in 2004 is evident in Figure 2. Although OTR and XA identifier attributes are not included in FIRES, these wildfires did not affect the IA and BH escape data we used because they are relatively easy to extinguish.

The IA and BH escape data are zero-inflated and long-tailed (Figure 4). Estimates for the probabilities of IA and BH success and escape for the 1990 to 2015 period for the month of May are summarized in an emperical probability tree (Figure 5). During the 1990 - 2015 period, a total of 7,523 wildires arrived in Alberta during the month of May. Approximately 91% of these wildfires were initial attacked before they exceeded 2.0 ha in size (IA Success). Of these 6,698 IA success wildfires approximately 97% were contained (BH Success) by 1000 h the following day of their assessment. The probability of a wildfire arrival being successfully initial attacked (IA Success) and contained (BH Success) is about 89%.

The third and fourth branches in Figure 6 include the probabilities of those wildfires escaping BH and exceeding 200 and 500 ha in size. Only 74 of the 7,523 wildfires in May grew larger than 500 ha in size. Such wildfires are costly and challenging for wildfire management agencies to control. For the same period (1990 - 2015) the month of April in comparison, had only 7 wildfires that grew larger than 500 ha in size. This follows the Pareto Principle (Pareto 1906)

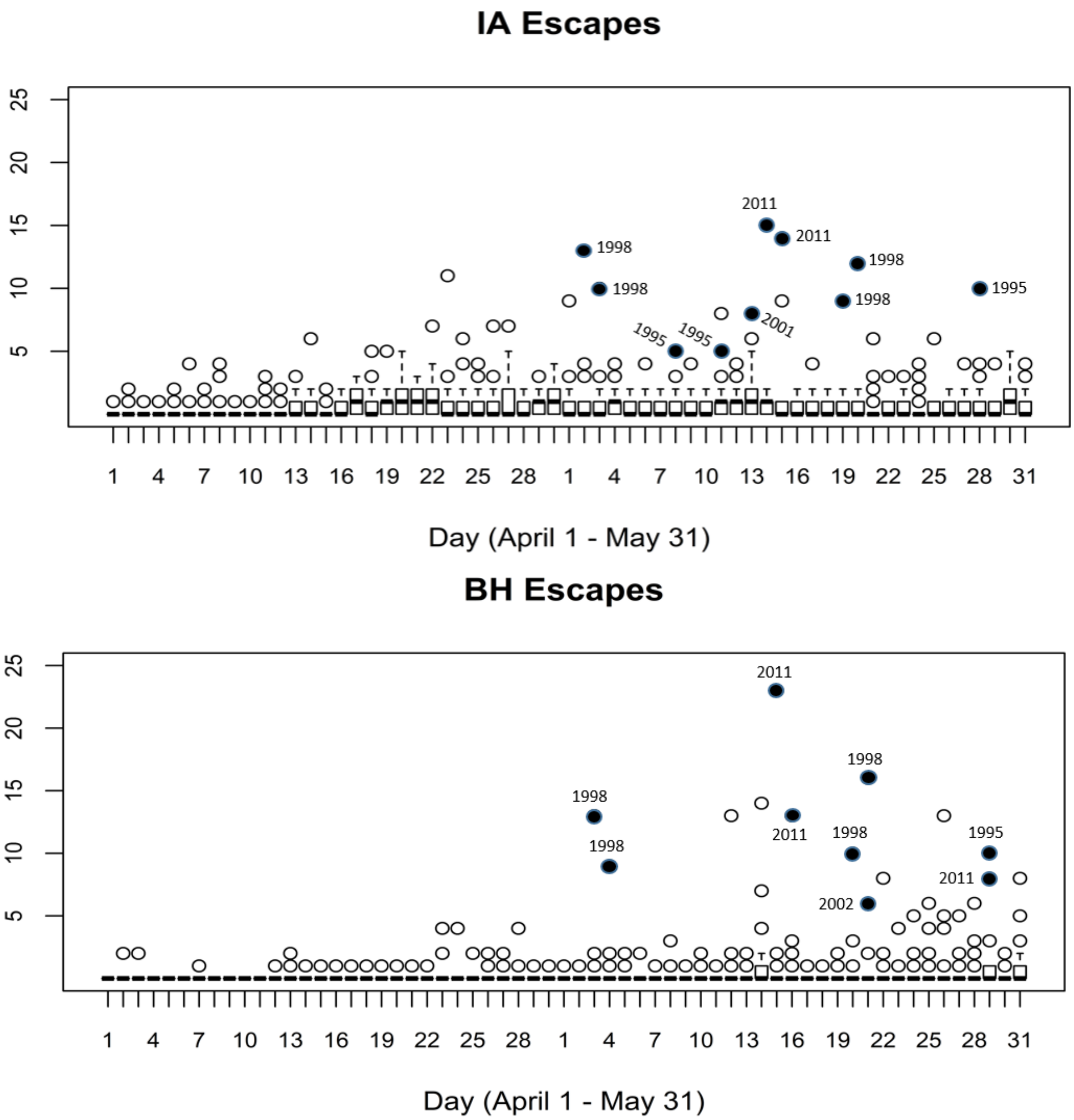

Figure 5: Boxplots of daily IA and BH escapes in Alberta for April and May 1990 - 2015. The years with the highest total area burned (refer to Figure 2) that had more than 4 daily IA escapes and more than 5 BH escapes are labeled and identified as black outliers.

where a small number of wildfires escape and cause the most impact. Later, we present the results of fitting parametric models for the IA and BH escape distributions, and illustrate a simple technique for syndromic surveillance based on the quality control literature.

2.2. El Niño Southern Oscillation Teleconnections

Besides the need to develop syndromic surveillance methods for near real-time monitoring for tactical wildfire management decision support there is also a strong need to identify

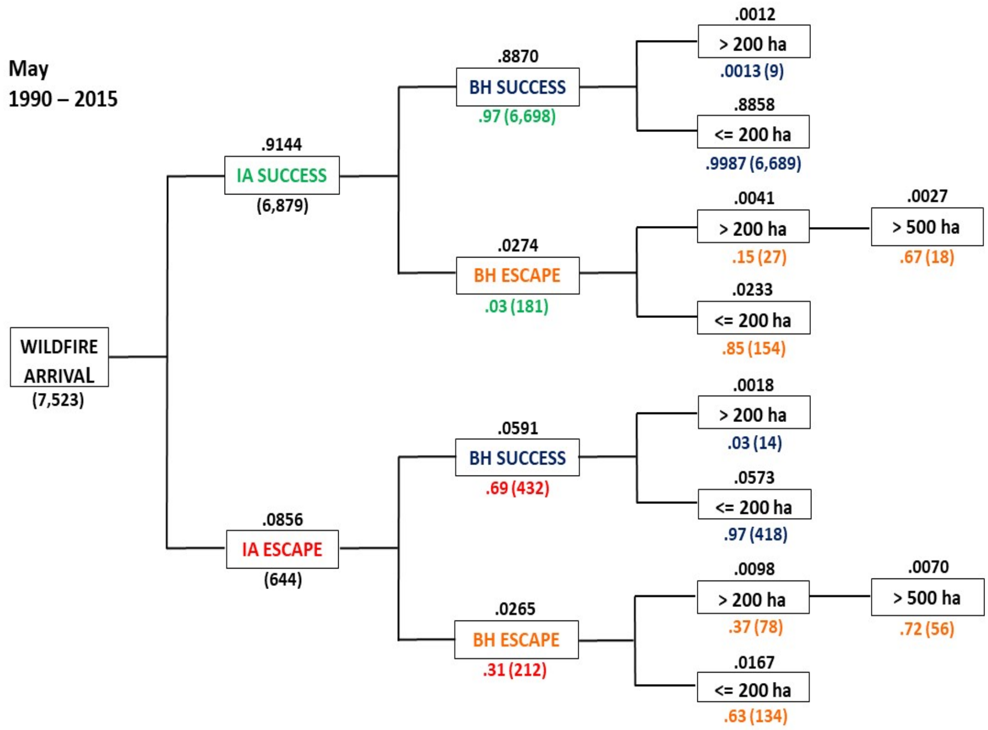

Figure 6: Emperical probability tree for May wildfire Initial Attack (IA) and Being Held (BH) successes and escapes for the period 1990-2015 when 7,523 wildfire arrivals were reported in Alberta for the month of May. Joint probabilities are given above each box, and group (by colour) probabilities and number of successes and failures are given below each box.

longer-term warning systems to support more strategic decisions such as seasonal staffing and the hiring of contract wildfire suppression aircraft. We thus obtained monthly sea surface temperature (SST) anomalies for an area in the Pacific Ocean referred to as Region 3.4 (5° N - 5° S, 120° - 170° W) from the United States National Weather Service Climate Prediction Center `http://www.cpc.ncep.noaa.gov/products/analysis_monitoring/ensostuff/detrend.nino34.ascii.txt`. The anomalies are the departures from the climatological monthly means for the 1981 - 2010 period. During strong El Niño events the warming of the central and east-central equatorial Pacific Ocean typically peaks during December (Trenberth 2016). We chose the December SST anomalies (°C) to indicate the likely persistence of environmental conditions and wildfire activity in the spring.

Implementing advanced readiness such as the activation of fire bans and area closures, increasing detection efforts, and mobilization of suppression resources in anticipation of a wildfire threat is usually made when thresholds (i.e. indicators that prompt a response) are reached. These thresholds however, are based primarily on expert opinion. In what follows we describe two approaches that can be used to develop early warning products in addition to the CFFDRS outputs to trigger advanced preparation to manage the impacts of a potential disastrous wildfire event.

3. Methods

3.1. IA and BH Escapes

We consider wildfire starts as akin to the arrivals of customers or patients that need servicing. The wildfire management response to wildfire arrivals can therefore be viewed as a process with associated quality or process control (i.e. IA and BH objectives). We investigated the various statistical process control (SPC) charts used in health-care (Woodall *et al.* 2012) for their application to the wildfire management response process. Quality control charts for count type data use statistical model parameters to set upper and lower thresholds called control limits, to identify when a process is not in control (Montgomery 2013). The time series surveillance approach with control limits that we use is similar to an attribute control chart (c-chart) with a constant size inspection unit. Our inspection unit is the entire population for a province-day. Since the lower control limit is not of concern to wildfire managers we only estimate the upper control limit.

We focused on detecting aberrations (outliers) in the number of IA and BH escapes during the months of April and May for the 1990 - 2015 period (Figure 5) using daily counts, and rolling 2- and 3-day sums. Two years (2016 and 2017) were reserved for a post-evaluation of the threshold selection and theoretical operational decision support. The rolling 3-day sum accounts for the long weekends in April and May (Canadian statutory holidays). Sums were selected because they are easily interpreted by operational wildfire management staff.

To understand the underlying structure and distribution of our discrete data we used exploratory data analysis and parametric model fitting of the distributions and their tails. We fitted Poisson, Negative Binomial, Zero-Inflated Poisson (Figure 7), and Zero-Inflated Negative Binomial distributions to the IA and BH count escape data. Since our data are zero-inflated and over dispersed, and because our objective is to derive operational early-warning thresholds of spring wildfire activity, we chose to apply univariate extreme value theory (EVT) and the Pareto Principle using the peak over threshold (POT) approach to model IA and BH escape risk. Introduced by Goda (1985), the POT technique models exceedances (peaks) of high, predetermined thresholds, and approximates the distribution of these right-tail outliers using the generalized Pareto distribution (GPD) (Balkeman and de Haan 1974; Pickands 1975). The cummulative denisty function of GPD is defined as:

$$F(x) = 1 - \left(1 + \frac{\xi x}{\sigma}\right)^{\frac{-1}{\xi}}$$

where $\sigma > 0$ and $\xi \in \mathbb{R}$ are scale and shape parameters and x is the distance above the predetermined exceedance threshold of interest. There are three forms of Pareto distribution to characterize the behaviour of extremes: Gumbel ($\xi = 0$), Frechét ($\xi > 0$) and Weibell ($\xi < 0$).

We applied the POT technique to estimate statistical surveillance thresholds using the R package POT (Ribatet 2019). The threshold exceedances were then fit to a GPD using the maximum likelihood estimation (MLE) method in the R package evir (Pfaff 2018). This approach allows for the calculation of IA and BH estimates and confidence intervals for various quantile and confidence levels.

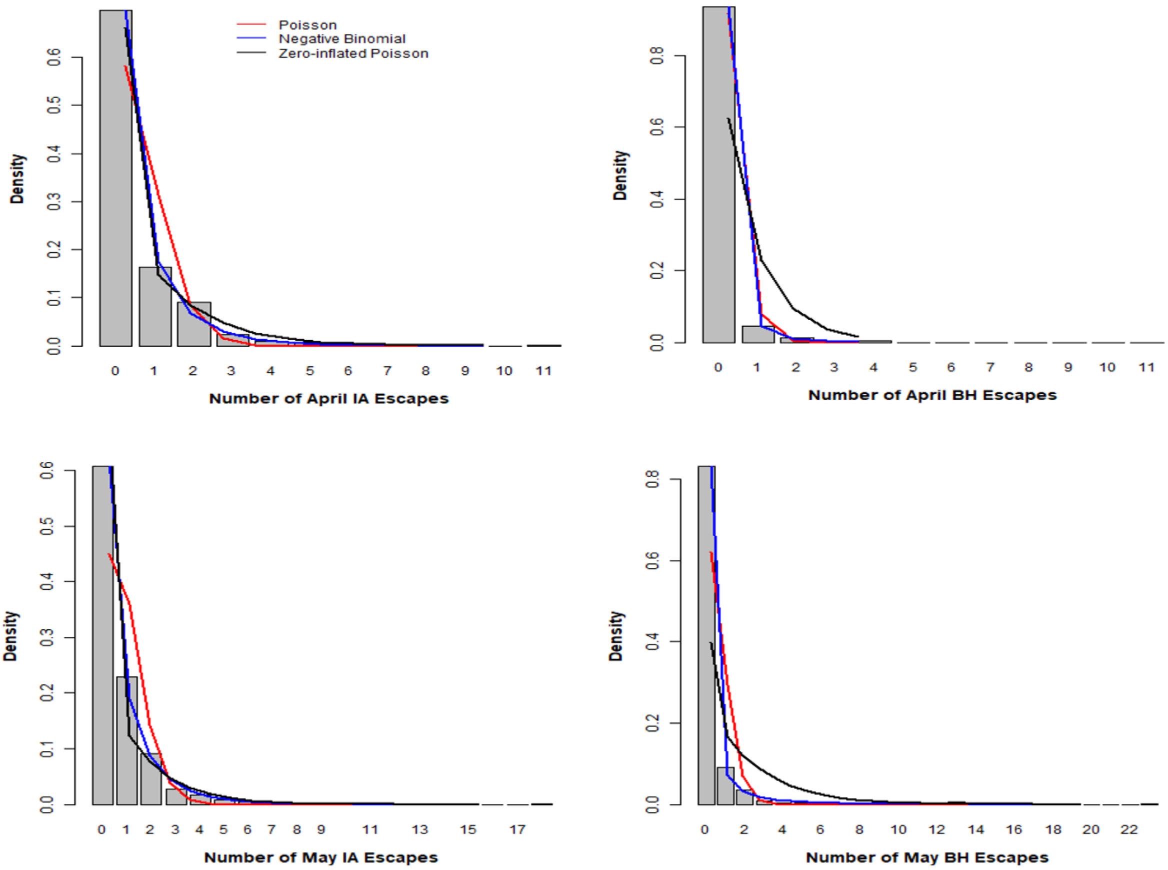

Figure 7: Poisson, Negative Binomial and Zero-inflated Poisson fit to the April (top) and May (bottom) IA (left) and BH (right) escape data for the 1990 - 2015 period.

As indicated, the POT approach requires one to set an excedance threshold. Although the POT package includes several functions for threshold estimation we chose percentiles, and the kurtosis method proposed by Patie (2000) to estimate IA and BH escape thresholds. Chen *et al.* (2015) used this kurtosis method to estimate threshold values for influenza outbreaks. The percentile levels we chose for our exploratory POT analyses were based on the 68-95-99.7 emperical rule. We include percentile thresholds as potential alternates to using thresholds based on the kurtosis since they are straightforward for end users to identify and associate with upper control limits.

Kurtosis and skewness are nonnormality measures of a distribution's "tailedness" and "asymmetry" respectively (Groeneveld and Meeden 1984). We are interested in the number of IA and BH escape extreme values that are outside of the normal range (i.e. a kurtosis value larger than that associated with a normal distribution). Univariate normal distributions have a Pearson's kurtosis value of 3. Kurtosis minus 3 refers to the excess kurtosis from an expected re-scaled value of 0 for the normal distribution. Excess kurtosis is defined as:

$$\hat{k} = \frac{\sum_{i=1}^{N} \frac{(X_i - \bar{X})^4}{n-1}}{s^4} - 3$$

where X_i is the i^th X value, $\bar{X}$ is the mean, s is the sample standard deviation, and n is the sample size.

Skewness is defined as:

$$S_k = 3\frac{(\bar{X} - \tilde{X})}{s}$$

where $\tilde{X}$ is the median.

To calculate thresholds using the kurtosis method, we applied four steps to each of our 24 datasets (see Tables 1-2). Excess kurtosis β_2, skewness μ_n and variance s_n^2 were first calculated. In the second step the observation of X_i maximizing $(X_i - \mu_n)^2$ was removed. The first and second steps were repeated until the excess kurtosis for the data subset was less than 3. The largest remaining X_i in the data subset was then chosen as the threshold.

3.2. El Nino Southern Oscillation Teleconnections

To supplement the nowcasting of IA and BH escape thresholds and provide additional situational awareness we also investigated the use of teleconnections data to provide a persistence forecast of the wildfire environment conditions. We plotted the December sea surface temperature anomaly for Region 3.4 in the equatorial Pacific Ocean from 1960 to 2017 (Figure 8). Since our IA and BH escape data are not normally distributed we used an ordinal measure of association to test our hypothesis that a positive teleconnection association exists between early and late spring wildfire activity. The Spearman Rank Correlation Coefficient (Spearman's ρ) was used to determine the strength of nine associations (ρ) of wildfire activity (number of wildfires and area burned) between various combinations of time periods in the spring (month and half month periods) and the December SST anomalies (°C) for Region 3.4 in the equatorial Pacific Ocean. The very strong (> 1.99 °C), strong (1.5 - 1.99 °C) and moderate (1.0 - 1.49 °C), weak (0.5 - 0.99 °C) categories of SST anomalies (Null 2018) were used to filter and recalculate Spearman's ρ for 9 of the 28 years when a warming ENSO event occurred.

To continue this exploratory data analysis, scatterplots (Figure 9) were made for selected associations with higher reported Spearman's ρ (number of wildfires in April versus May, number of BH escapes in April versus May, number of BH escapes in April period 2 versus the number of BH escapes in May period 1, and the number of BH escapes in May period 1 versus period 2). The April period 1 includes days 1 to 15, and period 2 includes days 16 to 30. The May period 1 includes days 1 to 15 and period 2 includes days 16 to 31.

4. Results

4.1. Model fitting

The May data set (31 days/26 years = 806 observations) included 643 IA escapes and 383 BH escapes. The score test for zero inflation (van den Broek 1995) indicated these data sets have significantly more zeros compared to the expected number of zeros from a Poisson distribution. This test statistic has a χ_1^2 distribution. The April data set (30 days/26 years =

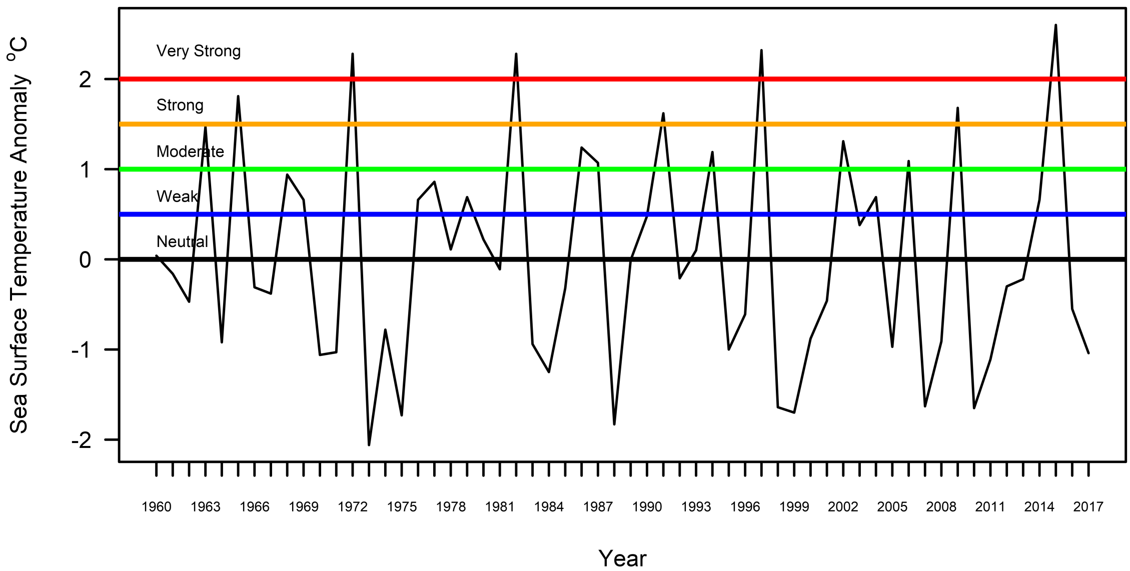

Figure 8: December sea surface temperature anomaly for Region 3.4 in the equatorial Pacific Ocean 1961 - 2017.

780 observations) included 422 IA escapes and 67 BH escapes. All corresponding upper tail p-values were $< .001$. We therefore fitted the four data sets to a zero-inflated Poisson (ZIP) distribution (Figure 7). We used Pearson's χ^2 test to assess the goodness-of-fit. The count IA and BH escape data for both April and May did not fit a ZIP distribution (Figure 7). All upper tail p-values were again $< .001$.

To address over-dispersion we fitted our count data to negative binomial and zero-inflated negative binomial distributions. These fits, however, also failed the goodness of fit test with all reported p-values $< .001$. We did not include the zero-inflated negative binomial fits in Figure 7 because they were so poor fits to these data. Q-Q plots of the resulting fits suggested a lack of fit in the upper tail of these distributions, and the need to model the tails using an extreme value distribution. We chose the generalized Pareto distribution (GPD) and peak over threshold approach.

Varying thresholds were calculated depending on the method used (Tables 1, 2). In our opinion the thresholds for the daily and 2- and 3-day rolling sum IA escape data (with zeros) based on the kurtosis method, and the BH escape data (with zeros) based on the 97 percentile method (Tables 1,2) are reasonable because they are supported by wildfire operations experts, and capture those years with severe spring wildfire activity (i.e. 1995, 1998, 2001, 2002, 2011). The calculated May threshold of 10 using the kurtosis method for the 3-day rolling sum of IA escapes resulted in 28 exceedances (Table 1). Threshold values of 9 and 11, in comparison yielded 35 and 21 exceedances respectively. Of the three percentiles, the 95 percentile resulted in IA escape thresholds that were closest to the thresholds calculated using the kurtosis method.

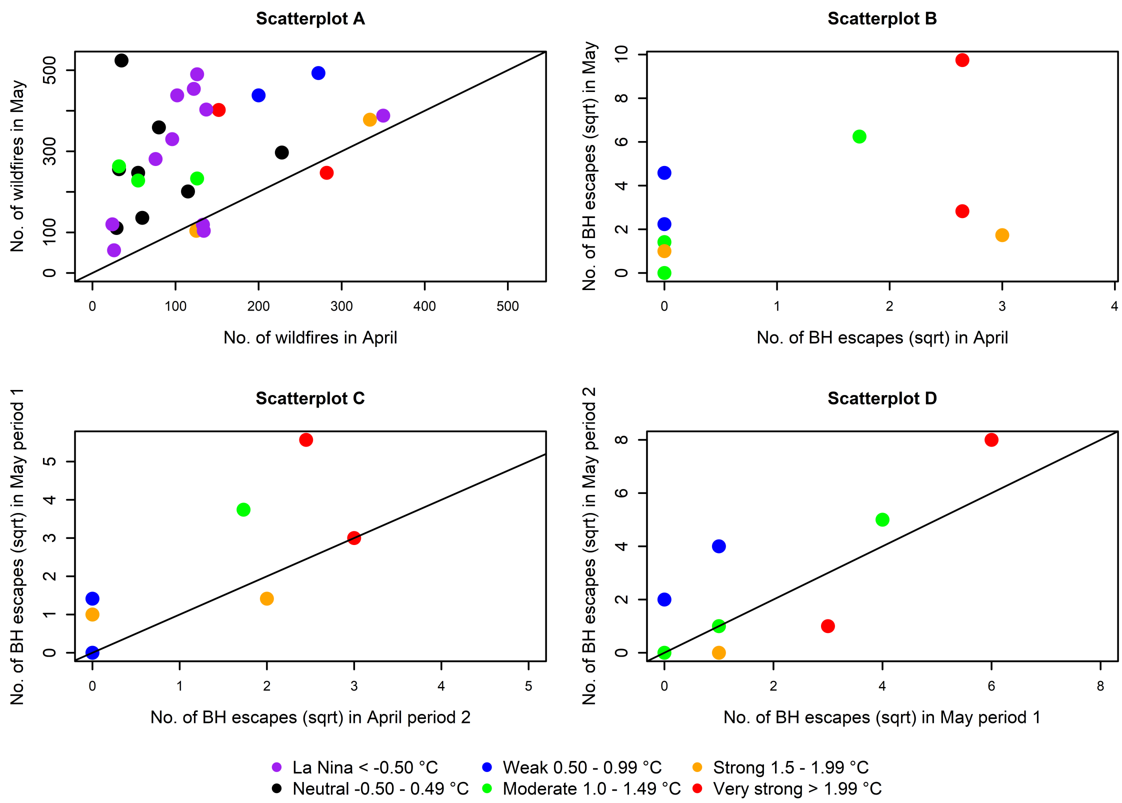

Figure 9: Scatterplots of spring wildfire activity in Alberta (1990 - 2017) with December sea surface temperature (SST) anomaly categories. The number of wildfires in April are plotted versus the number of wildfires in May in Scatterplot A. Scatterplots B, C, and D graph square root transformations of the variables. The number of BH escapes (sqrt) in April are plotted versus the number of BH escapes (sqrt) in May (Scatterplot B). Scatterplots C and D plot the number of April and May BH escapes for two different time periods.

The exceedances data based on a May IA escape threshold value of 10 fit the GPD distribution well as shown in the QQ plot of residuals (Figure 10). The maximum likelihood estimates of the scale and shape parameters are 9.77 (se = 2.86) and -0.363 (se = 0.23). The 95% CI for these parameters are 4.15 to 15.38 (scale), and -0.88 to 0.09 (shape). We acknowledge that rolling sums are inherently less noisy and fit better than the daily observations. All six QQ plots of residuals from the GPD are good fits for the month of May, including the fit to the daily observations (Figure 10).

We are unable to include similar QQ plots for April due to insufficient data being available to fit the GPD model to IA and BH escapes in that month. We note that, historically, there is much lower wildfire activity in April. This results in daily IA and BH escapes rarely occurring during this month and even when such an event does occur, its corresponding daily escape count is typically very small. This leads to a situation where there are very few threshold exceedances observed for a given threshold value identified by one of the methods and very little variability in the observed counts. Hence, the model cannot be fit. For example, a threshold value of three for BH escapes in April results in only three threshold exceedances

(Table 2). Note that for each of these instances the corresponding BH escape count was exactly four. With very few observations and little-to-no variability between such observations it is not possible to fit the GPD model in such situations; many more years of data are needed.

IA Escapes	68 Percentile Threshold: Exceedances		95 Percentile Threshold: Exceedances		99.7 Percentile Threshold: Exceedances		Kurtosis Method Threshold: Exceedances	
	April	May	April	May	April	May	April	May
IA escapes with zeros	0: 235	1: 130	2: 37	3: 37	7: 1	14: 2	3: 18	3: 37
IA escapes with no zeros	2: 38	2: 58	4: 11	6: 12	8: 1	15: 1	5: 6	5: 16
2-day rolling sum IA escapes with zeros	1: 209	2: 154	4: 32	6: 35	11: 3	21: 2	6: 16	8: 26
2-day rolling sum IA escapes with no zeros	3: 60	3: 98	6: 16	9: 16	13: 1	22: 2	8: 7	8: 26
3-day rolling sum IA escapes with zeros	2: 188	2: 241	5: 39	9: 35	15: 2	26: 3	9: 10	10: 28
3-day rolling sum IA escapes with no zeros	3: 114	3: 166	7: 20	10: 28	18: 2	28: 2	11: 8	12: 19

Table 1: Initial attack escape thresholds and threshold exceedances for April and May (1990 - 2015).

BH Escapes	68 Percentile Threshold: Exceedances		95 Percentile Threshold: Exceedances		99.7 Percentile Threshold: Exceedances		BH Objective (97 Percentile): Threshold Exceedances		Kurtosis Method Threshold: Exceedances	
	April	May	April	May	April	May	April	May	April	May
BH escapes with zeros	0: 48	0: 135	1: 13	2: 33	3: 3	14: 2	1: 13	4: 22	NaN	NaN
BH escapes with no zeros	1: 13	2: 33	3: 3	13: 3	4: 0	20: 1	4: 0	13: 3	3: 3	4: 22
3-day rolling sum BH escapes with zeros	0: 119	0: 257	2: 16	8: 36	5: 2	32: 3	2: 16	13: 23	NaN	3: 68
3-day rolling sum BH escapes with no zeros	2: 16	3: 68	4: 4	16: 13	6: 0	36: 1	4: 4	23: 7	5: 2	7: 41
2-day rolling sum BH escapes with zeros	0: 86	0: 206	1: 28	5: 35	4: 1	24: 2	2: 9	8: 24	NaN	NaN
2-day rolling sum BH escapes with no zeros	2: 9	2: 62	4: 1	15: 9	5: 1	30: 1	4: 1	17: 6	4: 1	7: 26

Table 2: Being held escape thresholds and threshold exceedances for April and May (1990 - 2015).

Since the kurtosis method resulted in very few threshold exceedances for BH escapes in April, and low threshold values with high numbers of exceedance for BH escapes in May, we added a fourth percentile level (0.97) as noted in Table 2. The Wildfire Management Branch in Alberta reported one performance metric in their Department's 2017-18 Annual

Report (Government of Alberta 2018b) called the Containment of Wildfires Performance Measure. This performance target is based on the previous five year average of the actual BH achievements. For example, the 2017 target was 97% (2012 - 2016 average), and the actual level achieved that year was 96.8%.

The calculated May threshold of 13 using the 97 percentile for the 3-day rolling sum of BH escapes resulted in 23 exceedances (Table 2). Threshold values of 12 and 14, in comparison yielded 35 and 21 exceedances respectively. The exceedances based on a threshold of 13 also fit the GPD distribution (Figure 10) with scale and shape parameters of 10.57 and -0.28 respectively.

We calculated quantile point estimates using a 95% confidence interval for the IA and BH threshold exceedances. The 0.98 quantile estimate of May IA escapes (3-day rolling sum) is 17.48 with lower and upper confidence intervals of 16.01 and 20.87. This estimate occurs once in about nine years. The 0.97 quantile estimate of May BH escapes (3-day rolling sum) is 22.99 with lower and upper confidence intervals of 19.68 and 28.25. This estimate also occurs once in about nine years.

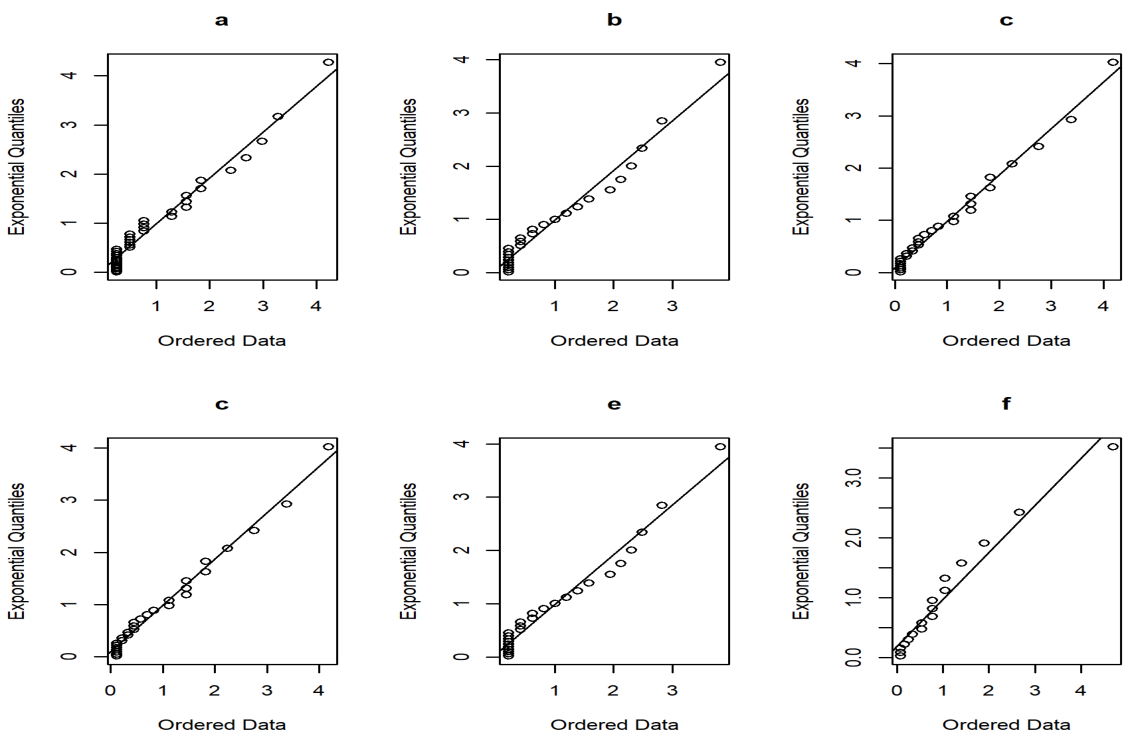

Figure 10: QQ plots of residuals for fitting the GPD to 1-, 2-, and 3- day IA (plots a, b, c) and BH (plots d, e, f) escapes in May. Plots a, b, and c use thresholds of 3, 8, and 10 respectively based on the Kurtosis method (with zeros). Plots d, e, and f use thresholds of 4, 8, and 13 respectively based on the percentile method (with zeros).

We focus our results on the month of May because it is a more critical month than April. On average only 7% of the days in April have one or more BH escapes. Higher extreme values of daily BH escapes occur in May (max = 23) compared to April (max = 6). More BH escapes occur in May because wildfires in April are usually easier to contain because of higher fuel moisture levels. The daily BH/IA escape ratio increased from 0.19 in April to 0.60 in May.

The extreme outliers of daily IA and BH escapes in Figure 4 show a buildup that begins at the start of May, peaks during the snow-melt to start of green-up period (second to third week of May), and tapers during the last week of May when green-up occurs.

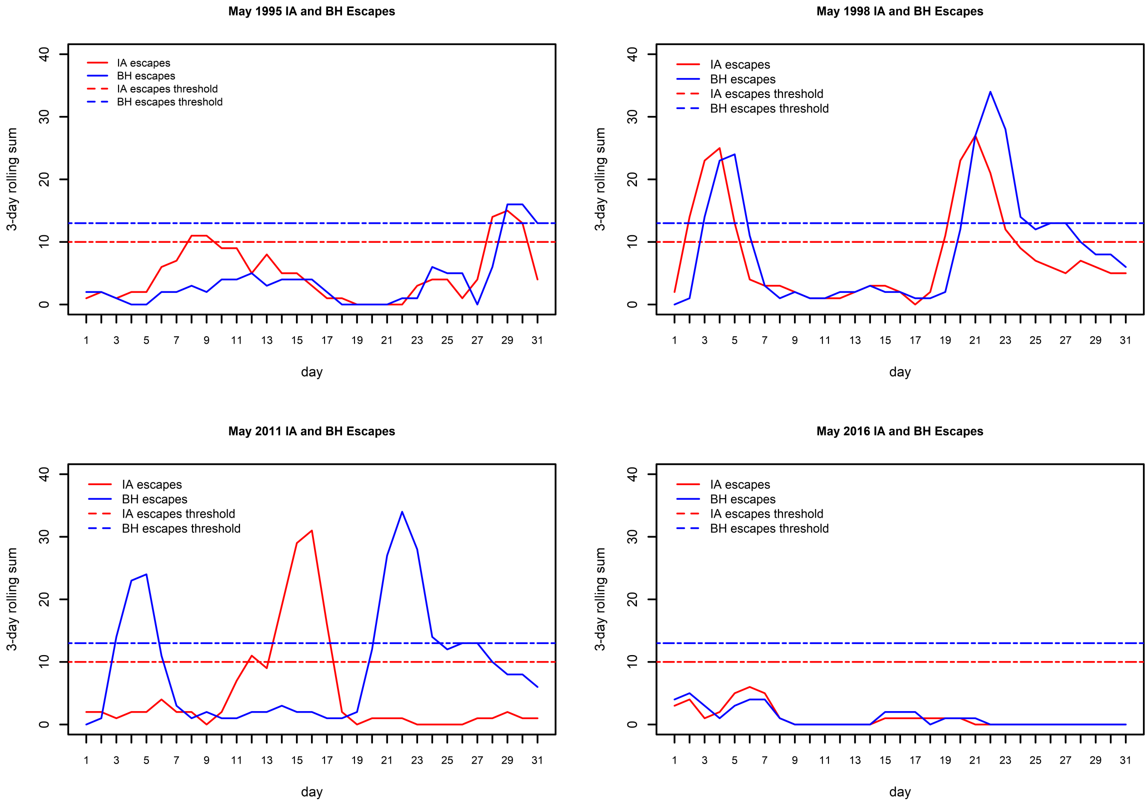

Figure 11: Rolling 3-day sum of IA escapes in May for 1995, 1998, 2011, and 2016 with corresponding threshold lines.

Figure 11 includes IA and BH escape charts for 1995, 1998, 2011, and 2016. Two years (2016 and 2017) were reserved for post-evaluation; 2017 was excluded from Figure 11 because like 2016 the IA and BH escapes did not surpass the thresholds. This in itself supports situational awareness but no early warnings are evident during 2016 and 2017 using the thresholds calculated based on the 1990 - 2015 peiod. However, examples of early warning for other years are evident in Figure 11. Alberta had a disastrous spring wildfire season in 1995. The plotted May 1995 IA escapes show a ramp up period before the 3-day sum peaked on May 8. This is an example of early warning. Another early warning is evident just before the second 3-day sum peak on May 29. The number of 3-day sum BH escapes in comparison do not exceed the threshold until May 29 indicating that most earlier wildfires were contained by 1000 h the following day.

In 1998 there was no early nowcast warning when the daily BH escapes peaked on May 3 (13 escapes) and May 21 (16 escapes). The second peak was coincident with the extended May holiday weekend and subsequent increase in recreational activities in the Forest Protection Area. The very strong El Niño that occurred during the winter of 1997/98 continued into the spring and contributed to the disastrous spring wildfire season.

No El Niño event occurred during the 2010/11 winter yet the following spring wildfire season that followed was also disastrous due to the influence of a dry Arctic high pressure system and accompanying strong southeast winds. An early warning is evident on May 11. This early warning when combined with the occurrence of a very strong El Niño during the winter of 1997/98, indicated the persistence of very high to extreme environment conditions and likely upward trend in spring IA and BH escapes. During the first week of May, wildfires were successfully initial attacked but they could not be contained.

Spearman Rank Correlation Coefficient 1990 – 2017	**ρ n = 28**	**ρ n = 9**
Number of wildfires in April vs Number of wildfires in May	0.38	0.52
Number of wildfires in April (> 4 ha) vs Number of wildfires in May (> 4 ha)	0.06	0.53
Area burned (ha) in April vs Area burned (ha) in May	0.16	0.32
Number of IA escapes in April vs Number of IA escapes in May	0.08	0.26
Number of BH escapes in April vs Number of BH escapes in May	0.40	0.47
Number of IA escapes in April Period 2 vs Number of IA escapes in May Period 1	.001	0.32
Number of BH escapes in April Period 2 vs Number of BH escapes in May Period 1	0.51	0.80
Number of IA escapes in May Period 1 vs Number of IA escapes in May Period 2	0.20	0.62
Number of BH escapes in May Period 1 vs Number of BH escapes in May Period 2	0.38	0.71

Table 3: Spearman Rank Correlation Coefficient (ρ) of spring wildfire activity and December sea surface temperature anomaly in Region 3.4 in the equatorial Pacific Ocean, with a comparison of all twenty-seven years, and nine teleconnection filtered years. The ρ values in the highlighted cells are significant at $\alpha = 0.05$.

4.2. El Nino Southern Oscillation Teleconnections

The Spearman's ρ values in the highlighted cells in Table 3 are significant at $\alpha = 0.05$ significance level. The critical values for Spearman's ρ (one-tail) are 0.375 (n = 28) and 0.786 (n

= 9).

The number of BH escapes in May period 2 is associated by rank with the number of BH escapes in May period 1 for all years. This association however is stronger when the subset of years is used when moderate to very strong December SST anomalies occurred. There is also a positive association between the number of BH escapes in May period 2 and the number of BH escapes in May period 1.

We also used scatterplots to visually explore spring wildfire activity and December SST anomalies. Four associations of spring wildfire activity are included in Figure 10. The x axis is the early time period and the y axis is the later time period. The December sea surface temperature anomaly categories are represented by colour (Purple = La Niña (< -05 °C), black = neutral (-0.50 - -0.49 °C), blue = weak (0.50 - 0.99 °C), green = moderate (1.0 - 1.49 °C), orange = strong (1.5 - 1.99 °C), and red = very strong (> 1.99 °C).

As expected, Scatterplot A (Figure 9) shows there are more wildland fires in May than in April. There are also no years with a high number of wildland fires in April followed by a low number of wildland fires in May. When the number of April wildland fires exceed 135, the following May wildland fires exceed 200 (mean = 380). Scatterplot C indicates the number of BH escapes in May period 2 is associated with the number of BH escapes in May period 1. No strong patterns are evident with the SST categories, other than the very strong El Niño events show wildland fire actvity in April persisting into May.

5. Discussion

During a full suppression response, wildfire management agencies aim to quickly keep wildland fire arrivals small in size. This is accomplished by determining the number, type, location and readiness status of suppression resources required in anticipation of the forecasted wildfire environment conditions and wildfire load for tomorrow (active wildfires plus new wildfire arrivals) (Martell 2001). Preparedness in Alberta is based on an 80% coverage objective (i.e. 80% of the forest area with forecasted Head Fire Intensity values (kW/m) greater than 10, must be reached by aerial or ground resources before a theoretical wildfire exceeds 2.0 ha in size) (Government of Alberta 2018a). Despite the planned rapid deployment of available resources using this consistent and objective approach, IA and BH escapes occur because very high to extreme environmental conditions support rapid wildfire growth and/or surges in wildfire arrivals. Fine fuel moisture and wind are the main variables contributing to large wildfire growth in the spring. One or two days of drying is sufficient to support rapid wildfire growth if accompanied by strong to extreme winds. IA and BH escapes are surrogate metrics of the environment and/or resource states (i.e. assignable cause). However, similar to control charts, surveillance charts do not assign the specific contributing cause of the process being out of control.

IA has the highest return on investment and is an immediate indicator of the wildfire and resource environments. However, we consider BH escapes as a stronger process control metric to provide situational awareness compared to IA escapes. If a wildfire cannot be contained by 1000 h the day following when the wildfire was assessed, the wildfire management effort transitions from IA to sustained attack. This phase usually demands more resources because the wildfire is typically larger and more intense. As shown in Figure 6, the arrival of IA resources on the a wildfire before it reaches 2 ha in size does not ensure BH success.

In Alberta, lightning-caused wildfires are relatively uncommon until the summer season begins. Historically, human activity causes 82% of the wildfires during May. Though further research is required, our analysis suggests that wildfire arrivals caused by human activity often occur in a ramp-up cluster pattern thereby providing early warning of potential increased wildfire activity. This pattern is typically not as evident with lightning-caused wildfire arrivals. As a result, IA and BH escape surveillance to track trends in threshold exceedances does not perform well to warn of sudden large surges of lightning-caused wildfire arrivals as happened in British Columbia in 2017 and 2018.

We foresee wildfire management duty officers having access to various statistical visualization charts to provide real-time firesurveillance of multiple metrics. These charts can provide evidence to support fire bans and area closures. Although we used monthly thresholds for the entire Province, these thresholds can be calculated and applied to administrative areas and ecoregions. Scotto *et al.* (2014) for example, characterized extreme daily area burned data and variability between districts in Portugal using a clustering analysis that combined the POT method and classification techniques. Shorter analysis time periods can also be used.

Wildfire management duty officers have considerable information to process. This includes what is happening on the entire landscape. The 2017 spring wildfire season was for example, quiet (Figure 11) but in the previous year Alberta experienced a devastating wildfire season when the Horse River Wildfire (MWF-009) started on May 1 and a few days later burned into Fort McMurray. A very strong El Niño event occurred in the 2015/16 winter and continued into the spring. Eight wildfires occurred in the Fort McMurray Forest Area before the Horse River Wildfire started. Three of the four wildfires reported within the Regional Municipality of Wood Buffalo occurred within the Fort McMurray Urban Service Area. Municipal wildfire MMD-002 on April 29 challenged firefighting resources from both the Fort McMurray Fire Department and Alberta Wildfire. This wildfire in particular was an early warning of the potential wildfire behaviour. Municipal wildfires are not entered in FIRES unless resources are requested from Alberta Wildfire. This incident highlights the importance of using all wildfires for surveillance and situational awareness. It also showed how even one BH escape spring wildfire can challenge a wildfire management agency and cause a disaster. This is unlike biosurveillance where single influenza occurrences do not trigger a disaster.

Discrete extreme-value modeling for wildfire surveillance using IA and BH escape data is particularly challenging. There is little literature on the application of standard EVT for discrete extreme-value modeling. Anderson (1997) suggested that the maxima of Poisson counts can be reasonably estimated by using the generalized extreme value distribution conditional on having a large enough mean. Our means however are too small due to zero-inflation. We note that a discrete analogue of the generalized Pareto distribution (D-GPD) and the generalized Zipf distribution (GZD) proposed by Hitz *et al.* (2017) has been found to perform well to estimate discrete extremes. Prieto *et al.* (2014) used D-GPD to model road accidents in Spain. Despite the GPD not being a discrete distribution it reportedly performed well to estimate the probability of extreme events including extreme tornado outbreaks (Hitz *et al.* 2017). We therefore chose to use the Peak-over-threshold (POT) Generalized Pareto Distribution (GPD) to characterize our IA and BH escape data.

There is no standard method of threshold selection when using the POT approach. Lang *et al.*

(1999) provided an overview of the methods and challenges for modeling the POT process. We chose the percentile and Kurtosis methods because they are relatively objective, simple in their application, and Wildfire Management Branch in Alberta uses percentiles as part of a fire weather analysis toolkit in their FIRES system.

If the threshold is too high, the variance increases because of the lower number of exceedances. Likewise, if the threshold is too low, the GPD approximation is not accurate because too many non-extreme values induce bias. An automated selection method to estimate an optimum threshold as proposed by (Bader *et al.* 2018) may be the best approach to find a balance.

The very strong ENSO warm period in 2015/2016 contributed to the spring drought. The previous very strong ENSO warm period in 1997/1998 was also followed by a disastrous wildfire season in Alberta. A disastrous wildfire season did not follow the very strong ENSO warm period in 1982/1983. After three consecutive wildfire seasons with large areas burned in 1980, 1981 and 1982, Alberta implemented a new preparedness system which combined with fewer reported wildfire starts may have prevented a disastrous wildfire season in 1983. Although disastrous spring wildfire seasons are not dependent on an El Niño occurrence, these warming events contribute to drier wildfire environment conditions. Local conditions however may vary. Wildfires require three main ingredients: available fuel, ignition (human and lightning), and favourable weather conditions. Since there can be high spatial and temporal variability of weather and subsequent burning conditions it is difficult to identify local teleconnections (i.e. a specific location and short time period). We used December SST anomalies as a simple indicator of the potential persistence of spring wildfire activity. There are a suite of Northern Hemisphere teleconnection indices such as the Arctic Oscillation (AO) Index, Pacific Decadal Oscillation (PDO) Index, Pacific-North American (PNA) Index, and the Oceanic Niño (ONI) Index (National Oceanic and Atmospheric Administration 2018) that can be tracked individually or in combination Wang *et al.* (2014) for example, forecasted regional drought-flood changes based on the combined effect of ENSO and PDO.

6. Conclusion

We applied simple and operationally viable statistical approaches with visualization techniques commonly used in health sciences to enhance situational awareness of spring wildfire activity in Alberta. We suggest the Wildfire Management Branch implement IA and BH escape surveillance using the daily and 3-day rolling sum May IA escape thresholds of 3 and 10 respectively (kurtosis method), and the 3-day rolling sum May BH escape threshold (97 percentile) of 13.

Our exploratory data analysis and use of IA and BH escape surveillance charts with thresholds focused on the spring season but can be applied during the entire wildfire season, and for all phases of the wildfire cycle (Figure 4). When surveillance charts with multiple statistical thresholds are used with 10 - 14 day outlooks of wildfire occurrence and behaviour potential they can provide early warning of likely wildfire events by indicating the trend direction of IA and BH escapes. It is important to integrate nowcasting with forecasting because it can take two weeks to mobilize resources from outside Canada. Wildfire management agencies can also conduct early surveillance of ENSO data to provide a warning of wildfire environment conditions that are likely to persist in the spring. For example, the surveillance of BH escapes in April can be used to help plan for May, particularly during ENSO warming events, and when extended periods of drying are forecasted. Since every El Niño event is different (timing, length and strength), it is important to track them, particularly the very strong and strong ENSO warming events. Monthly SST anomalies can be tracked using the thresholds identified in Figure 8.

The syndromic surveillance of near-real time IA and BH escapes when combined with CFF-DRS and fire occurrence outputs allows wildfire management agencies the opportunity to consider mobilizing resources and activating prevention measures such as fire bans and area closures, in advance. Future work is required to investigate the use of other metrics including fire load and rate of IA and BH escapes, and the use of POT modelling with multivariate generalized Pareto distributions. Temporal and spatial multivariate thresholds can then, for example, be set based on escape rate, fire load and time period. Fire load was an important factor during the 2011 spring wildfire season. From May 11 - 15, 22 on-going fires and 189 new wildfire starts occurred. An early fire load surge on May 1 was an early warning of the potential wildfire activity the following week.

Wildfire disasters in Canada and globally are increasing. Wildfire managers therefore need the best available information and tools to support decision making. This requires innovative and integrated approaches to manage a future world with more wildfire. In particular, the application of advanced statistical approaches are desirable, but this necessitates the engagement and contribution from the statistical sciences community. This horizontal collaboration will help to inform how wildfire management agencies can be better prepared to manage wildfire events.

Acknowledgements

We thank the Alberta Department of Agriculture and Forestry for the use of the wildfire data. We acknowledge the support of the Natural Sciences and Engineering Research Council of Canada (NSERC), [funding reference number RGPIN-2015-04221], and the support of the Canadian Statistical Sciences Institute (CANSI) [Collaborative Research Team Project]. Canada Wildfire (Canadian Partnership for Wildland Fire Science) also provided funding for travel.

References

Abott G, Chapman M (2018). "Addressing the new normal 21st century disaster management in British Columbia.Natural catastrophes and man-made disasters in 2017: A year of record-breaking losses." *Report P-148*, Report and findings of the BC flood and wildfire review: an independent review examining the 2017 flood and wildfire seasons.

Anderson CW (1997). "Maxima of Poisson-like variables and related triangular arrays." *Annals of Applied Probability*, **7**(4), 953–971.

Bader B, Yan J, Zhang X (2018). "Automated threshold selection for extreme value analysis via ordered goodness-of-fit tests with adjustment for false discovery rate." *Annals of Statistics*, **12**(1), 310–329. doi:10.1214/17-AOAS1092.

Balkeman B, de Haan L (1974). "Residual life time a great age." *The Annals of Applied Statistics*, **2**(5), 792–804.

Beverly J, Flannigan MD, Stocks BJ, Bothwell P (2011). "The association between Northern Hemisphere climate patterns and interannual variability in Canadian wildfire activity." *Canadian Journal of Forest Research*, **41**(11), 2193–2201. doi:10.1016/j.ecolmodel.2008.12.007.

Chen J, Lei X, Zhang L, Peng B (2015). "Using extreme value theory approaches to forecast the probability of outbreak of highly pathogenic influenza in Zhejiang, China." *PLOS One*, **10**(2). doi:10.1371/journal.pone.0118521.

Das D, Metzger K, Heffernan R, Balter S, Weiss D, Mostashari F (2005). "Monitoring over-the-counter medication sales for early detection of disease outbreaks." *PubMed*, **54**(Suppl).

de Groot WJ, Wotton BM, Flannigan MD (2015). *Wildland fire danger rating and early warning systems*, chapter 11, pp. 207–228. Elsevier, Amsterdam, NL.

Earnest A, Tan SB, Wilder-Smith A, Machin D (2012). "Comparing statistical models to predict dengue fever notifications." *Computational and Mathematical Methods in Medicine*, **2012**(758674). doi:10.1155/2012/758674.

Endsley MR (1995). "Toward a theory of situation awareness in dynamic systems." *Human Factors Journal*, **34**(1), 32–64.

Fricker RD (2013). *Introduction to statistical methods for biosurveillance.* P-399. Cambridge University Press, Cambridge, UK.

Goda Y (1985). *Random seas and design of maritime structures.* P-323. The University of Tokyo Press, Tokyo, Japan.

Goldstein E, Cobey S, Takahashi S, Miller JC, Lipsitch M (2011). "Predicting the epidemic sizes of influenza A/H1N1, A/H3N2, and B: A statistical method." *PLOS Medicine*, **8**(7). doi:10.1371/journal.pmed.1001051.

Government of Alberta (2018a). "Standing Operations Procedures 2018." *Report P-582*, Alberta Agriculture and Forestry, Wildfire Management Branch.

Government of Alberta (2018b). "Agriculture and Forestry Annual Report 2017-2018." *Report P-165*, Alberta Agriculture and Forestry, Wildfire Management Branch.

Groeneveld RA, Meeden G (1984). "Measuring skewness and kurtosis." *Statistician*, **33**(4), 391–399.

Hii YL, Zhu H, Ng N, Ng LC, Rockl\'ov J (2012). "Forecast of dengue incidence using temperature and rainfall." *PLOS Neglected Tropical Diseases*, **6**(11). doi:10.1371/journal.pntd.0001908.

Hitz A, Davis R, Samorodnitsky G (2017). "Discrete extremes." *Paper*, Cornell University Library.

Insurance Bureau of Canada (2017). "Facts of the property and causualty industry in Canada: 2017." *Report P-66*, Insurance Bureau of Canada.

Insurance Information Institute (2018). "Spotlight on: Catastrophes - Insurance issues." Accessed April 4, 2019, URL https://www.iii.org/rticle/spotlight-on-catastrophes-insurance-isses.

Kara EO, Elliot AJ, Bagnall H, Foord DGF (2011). "Absenteeism in schools during the 2009 influenza A(H1N1) pandemic: A useful tool for early detection of influenza activity in a community." *Epidemiology and Infection*, **140**(7). doi:10.1017/S0950268811002093.

Lagerquist R, Flannigan MD, Wang X, Marshall G (2017). "Automated prediction of extreme fire weather from synoptic patterns in Northern Alberta, Canada." *Canadian Journal of Forest Research*, **47**(9), 1175–1183. doi:10.1139/cjfr-2017-0063.

Lang M, Ouarda TBMJ, Bobée B (1999). "Towards operational guidelines for over-threshold modeling maxima of Poisson-like variables and related triangular arrays." *Annals of Applied Probability*, **225**(3-4), 103–117. doi:doi.org/10.1016/S0022-1694(99)00167-5.

Martell DL (2001). *Forest fire management*, chapter 15, pp. 527–583. Academic Press, San Diego, United States.

Montgomery DC (2013). *Introduction to statitical quality control*. P-754. Wiley, Hoboken NJ.

Mugglin AS, Cressie N, Gemmell I (2002). "Hierarchical statistical modelling of influenza epidemic dynamics in space and time." *Statistics in Medicine*, **30**(21), 2703–21. doi:10.1002/sim.1217.

National Oceanic and Atmospheric Administration (2018). "Climate Indices: Monthly Atmospheric and Ocean Time Series." https://www.esrl.noaa.gov/psd/data/climateindices/list/. Accessed: 2018-09-30.

Natural Resources Canada (2018). "Canadian Wildland Fire Information System Datamart: National Fire Database fire point data." Accessed June 4, 2018, URL https://cwfis.cfs.nrcan.gc.ca/datamart.

Null J (2018). "El Niño and La Niña years an intensities." https://ggweather.com/enso/oni.htm. Accessed: 2018-09-30.

Pareto V (1906). *Manuale di economia politica con una introduzione alla scienza sociale.* P-579. Societá Editrice Libreria, Milano, Italy.

Patie P (2000). "Estimation of value at risk using extreme value theory." *Working paper, cited 10 June 2014 in: Talks in financial and insurance mathematics, Department of Mathematics, ETH Zurich.*

Pfaff B (2018). *Extreme Values in R.*

Pickands J (1975). "Statistical inference using extreme order statistics." *The Annals of Statistics*, **3**, 119–131.

Pickell PD, Coops NC, Ferster CJ, Bater CW, Blouin KD, Flannigan MD, Zhang J (2017). "An early warning system to forecast the close of the spring burning window from satellite-observed greenness." *Scientific Reports*, **7**(14190). doi:10.1038/s41598-017-14730-0.

Preisler H, Brillinger DR, Burgan RE, Benoit JW (2004). "Probability based models for estimation of wildfire risk." *International Journal of Wildland Fire*, **13**(2), 133–142. doi:10.1071/WF02061.

Prieto F, Gómez-Déniz E, Sarabia JM (2014). "Modelling road accident blackspots data with the discrete generalized Pareto distribution." *Accident Annalysis Prevention*, **71**, 38–49.

Public Safety Canada (2018). "The Canadian Disaster Database." https://www.publicsafety.gc.ca/cdd. Accessed: 2018-09-30.

Rasmusson EM, Wallace JM (1983). "Meteorological aspects of El Niño/Southern Oscillation." *Science*, **222**((4629)), 1195–1202. doi:10.1126/science.222.4629.1195.

Ribatet M (2019). *An R package for univariate and bivariate peaks over threshold analysis.*

Scotto MG, Gouveia S, Carvalho A, Monteiro A, Martins V, Flannigan M, San-Miguel-Ayanz J, Miranda AI, Borrego C (2014). "Area burned in Portugal over recent decades: an extreme value analysis." *International Journal of Wildland Fire*, **23**(6), 812–824.

Shabbar A, Skinner W, Flannigan W (2011). "Prediction of seasonal forest fire severity in Canada from large-scale climate patterns." *Journal of Applied Meteorology and Climatology*, **50**(4), 785–799.

Shi Y, KoK SY, Rajarethinam J, Liang S, Yap G, Chong CS, K-S Lee SSYT, Chin CKW, Lo A, Kong W, Cook AR (2016). "Three-month real-time dengue forecast models: An early warning system for outbreak alerts and policy decision support in Singapore." *Environmental Health Perspectives*, **124**(9). doi:10.1289/ehp.1509981.

Skinner WR, Shabbar A, Flannigan W, Logan K (2006). "Large forest fires and the relationship to global sea surface temperatures." *Journal of Geophysical Research*, **111**((D14106)). doi:10.1029/2005JD006738.

Soebiyanto RP, Adimi F, Kiang RK (2010). "Modeling and predicting seasonal influenza transmission in warm regions using climatological parameters." *PLOS Medicine*, **5**(3). doi:10.1371/journal.pone.0009450.

Stocks BJ, Lawson BD, Alexander ME, van Wagner CE, McAlpine RS, Lynham TJ, Dube DE (2002). "Canadian Forest Fire Danger Rating System." *The Forestry Chronicle*, **65**(4), 258–265.

Stocks BJ, Lawson BD, Alexander ME, Wagner CEV, McAlpine RS, Lynham TJ, Dube DE (1989). "Canadian Forest Fire Danger Rating System." *The Forestry Chronicle*, **65**(4), 258–265.

Swiss Re Institute (2018). "Natural catastrophes and man-made disasters in 2017: A year of record-breaking losses." *Report P-50*, Swiss Re Institute.

Taylor SW, Woolford DG, Dean CB, Martell DL (2013). "Wildfire prediction to inform fire management: Statistical science challenges." *Statistical Science*, **28**(4). doi:10.1214/13-STS451.

Thomson MC, Mason SJ (2012). "Malaria early warnings based on seasonal climate forecasts from multi-model ensembles." *Nature*, **439**(7076). doi:10.1038/nature04503.

Trenberth K (2016). "What North America can expect from El Niño." https://theconversation.com/what-north-america-can-expect-from-el-nino-51959. Accessed: 2018-09-30.

Tymstra C (2015). *The Chinchaga Firestorm: When the moon and sun turned blue*. P-233. The University of Alberta, Edmonton, Alberta, Canada.

van den Broek J (1995). "A score test for zero inflation in a Poisson distribution." *Biometrics*, **51**(2), 738–743.

Van Wagner CE (1967). "Seasonal variation in moisture content of eastern Canadian tree foliage and the possible effect on crown fires." *Report 1204*, Department of Forestry and Rural Development.

Wang A, Huang J, He Y, Guan Y (2014). "Combined effects of the Pacific Decadal Oscillation and El Niño-Southern Oscillation on global land dry-wet changes." *Scientific Reports*, **4**((6651)). doi:doi:10.1038/srep06651.

Wang Y, Flannigan M, Anderson K (2010). "Correlations between forest fires in British Columbia, Canada, and sea surface temperature of the Pacific Ocean." *Ecological Modelling*, **221**(1). doi:doi:10.1016/j.ecolmodel.2008.12.007.

Woodall WH, Adams BM, and JCB (2012). *The use of control charts in healthcare*, chapter 12, pp. 251–267. Wiley, Chincheater, ENG. doi:doi.org/10.1002/9781119940012.ch12.

Woolford DG, Flannigan MD, Wang X, Marshall G (2014). "Lightning-caused forest fire risk terns in northwestern Ontario, is increasing and associated with anomalies in fire weather." *Environmetrics*, **25**(6), 417–430. doi:10.1002/env.2278.

Yang YT, Homeffer M, DiLisio N (2013). "Mining social media and web searches for disease detection." *Journal of Public Health Research*, **2**(1). doi:10.4081/jphr.2013.e4.

Affiliation:

Cordy Tymstra
Department of Renewable Resources
University of Alberta
751 General Services Building
Edmonton, Alberta, Canada T6G 2H1
E-mail: cordy.tymstra@ualberta.ca